INORGANIC CHEMISTRY

FRONTIERS

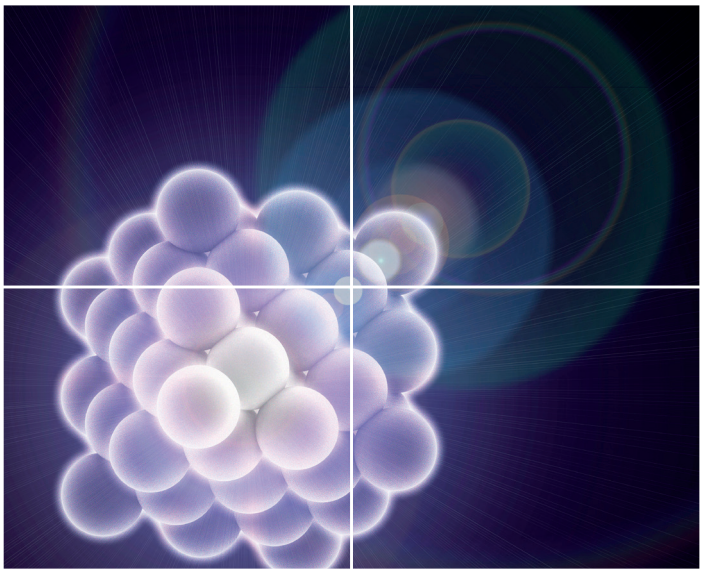

Accepted Manuscript

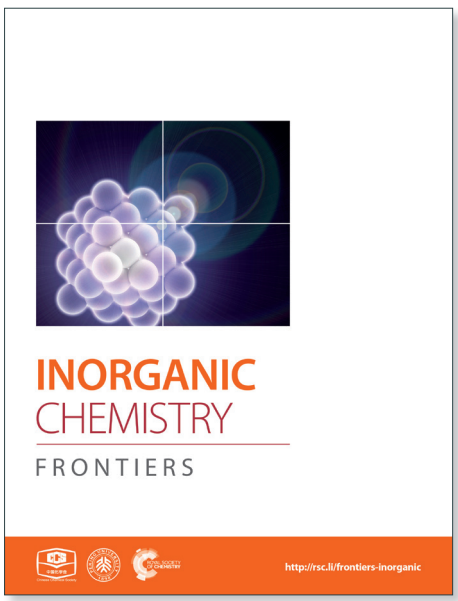

This is an *Accepted Manuscript*, which has been through the Royal Society of Chemistry peer review process and has been accepted for publication.

Accepted Manuscripts are published online shortly after acceptance, before technical editing, formatting and proof reading. Using this free service, authors can make their results available to the community, in citable form, before we publish the edited article. We will replace this *Accepted Manuscript* with the edited and formatted *Advance Article* as soon as it is available.

You can find more information about *Accepted Manuscripts* in the **Information for Authors**.

Please note that technical editing may introduce minor changes to the text and/or graphics, which may alter content. The journal's standard **Terms & Conditions** and the **Ethical guidelines** still apply. In no event shall the Royal Society of Chemistry be held responsible for any errors or omissions in this *Accepted Manuscript* or any consequences arising from the use of any information it contains.

Journal Name

RSCPublishing

ARTICLE

Macroscopic polarity control with alkali metal cation size and coordination environment in a series of tin iodates

Cite this: DOI: 10.1039/x0xx00000x

Received 00th January 2014,
Accepted 00th January 2014

DOI: 10.1039/x0xx00000x

www.rsc.org/

Yeong Hun Kim,[1] T. Thao Tran,[2] P. Shiv Halasyamani,[2] and Kang Min Ok[1,*]

A series of stoichiometrically similar tin(IV) iodates, $A_2Sn(IO_3)_6$ (A = Li, Na, K, Rb, Cs) and $Sn^{2+}Sn^{4+}(IO_3)_6$ have been hydrothermally synthesized. X-ray diffraction was used to determine the crystal structures of the reported materials. All six materials reveal zero-dimensional molecular structures that consist of SnO_6 octahedra and IO_3 polyhedra. However, the size and coordination environment of cations significantly influence the macroscopic centricities of the materials. While $Li_2Sn(IO_3)_6$ and $Na_2Sn(IO_3)_6$ crystallize in the noncentrosymmetric (NCS) polar space group, $P6_3$, the K, Rb, Cs, and Sn phases crystallize in the centrosymmetric (CS) nonpolar space group, R-3. Infrared and UV-vis spectroscopies, thermal analyses, and local dipole moment calculations are reported. With the NCS polar materials, powder second-harmonic generation (SHG) properties, polarization, and piezoelectric measurements are also presented. The NCS properties are mainly attributable to the parallel alignment of the lone pairs in I^{5+} cations.

Introduction

Molecular materials have been of broad and current interest attributable to their wide ranges of important applications in photonics, information processing, data storage, and nanotechnology.[1] Synthetic chemists have made continuous efforts to tune the characteristics of the materials by controlling the orientation and alignment of the molecules. Among many functional compounds, materials crystallizing in noncentrosymmetric (NCS) structures have drawn enormous attentions because of their technologically advanced properties, such as second-order nonlinear optical (NLO), piezoelectric, and multiferroic behaviors.[2] Especially, polar materials exhibiting permanent dipole moments along a specifically defined direction are of great interest attributed to their two unique properties, *i.e.*, pyroelectricity and ferroelectricity.[3-5] Although the two interesting properties are found from polar materials, ferroelectricity is only observed when a *switchable* polarization exists within the crystal. In other words, a ferroelectric is a pyroelectric material that has a reversible polarization. Two successful approaches to develop superior performing polar materials are the crystallographically ordered d^0 transition metal oxyfluorides[6-10] and oxides containing second-order Jahn-Teller (SOJT) distortive cations.[11-22] With the former, changes in the bond network notably influence different crystal polarities. With the latter, incorporating locally polar polyhedra, such as octahedrally coordinated d^0 transition metal cations and lone pair cations, into an extended backbone plays an important role in creating a macroscopic polar structure. In addition, a number of NCS polar materials have been observed from d^{10} transition metal cations revealing polar displacement as well as compounds composed of borate groups exhibiting unsymmetrical π-orbital systems.[23-27] However, those local asymmetric building units frequently fall into line in an antiparallel manner and result in centrosymmetric (CS) nonpolar structures. Therefore, it is more important to understand key factors deciding the crystallographic centricity through close structural examinations. A series of alkali metal titanium iodate materials, $A_2Ti(IO_3)_6$ (A = Li, Na, K, Rb, Cs, Ag), with zero-dimensional structures have been recently reported, in which the size of alkali metal cations affect significantly the overall polarity of the materials.[28-30] Other reported elements controlling the macroscopic polarity include the framework flexibility and the hydrogen bonding effect.[31-36] Here we report hydrothermal syntheses and thorough characterizations of six new stoichiometrically similar molecular tin iodates, $A_2Sn(IO_3)_6$ (A = Li, Na, K, Rb, Cs) and $Sn^{2+}Sn^{4+}(IO_3)_6$. We will demonstrate how the cation size and coordination environment influence the polarity of the materials. With the polar iodates, $Li_2Sn(IO_3)_6$ and $Na_2Sn(IO_3)_6$, detailed NCS functional properties, such as second-harmonic generation (SHG), piezoelectricity, and polarization measurements will also be reported.

Experimental

Syntheses

Li_2CO_3 (Hayashi, 98.0%), Na_2CO_3 (Hayashi, 99.5%), K_2CO_3 (Jin Chemical, 99.5%), Rb_2CO_3 (Alfa Aesar, 99.8%), Cs_2CO_3 (Aldrich, 99.0%), $SnCl_2$ (Alfa Aesar, 98%), and HIO_3 (Alfa Aesar, 99.0%) were used as received. Single crystals of the reported compounds have been obtained through hydrothermal reactions. For $Li_2Sn(IO_3)_6$, 0.185 g (2.50×10^{-3} mol) of Li_2CO_3, 0.119 g (6.25×10^{-4} mol) of $SnCl_2$, 5.940 g (3.38×10^{-2} mol) of HIO_3, and 10 mL of deionized water were combined. For $Na_2Sn(IO_3)_6$, 0.265 g (2.50×10^{-3} mol) of Na_2CO_3, 0.119 g (6.25×10^{-4} mol) of $SnCl_2$, 5.940 g (3.38×10^{-2} mol) of HIO_3, and 10 mL of deionized water were combined. For $K_2Sn(IO_3)_6$, 0.173 g (1.25×10^{-3} mol) of K_2CO_3, 0.119 g (6.25×10^{-4} mol) of $SnCl_2$, 1.320 g (7.50×10^{-2} mol) of HIO_3, and 5 mL of deionized water were combined. For $Rb_2Sn(IO_3)_6$, 0.289 g (1.25×10^{-3} mol) of Rb_2CO_3, 0.119 g (6.25×10^{-4} mol) of $SnCl_2$, 1.100 g (6.25×10^{-3} mol) of HIO_3, and 7.5 mL of deionized water were combined. For $Cs_2Sn(IO_3)_6$, 0.407 g (1.25×10^{-3} mol) of Cs_2CO_3, 0.237 g (1.25×10^{-3} mol) of $SnCl_2$, 1.650 g (9.38×10^{-3} mol) of HIO_3, and 7.5 mL of deionized water were combined. For $Sn^{2+}Sn^{4+}(IO_3)_6$, 0.053 g (5.00×10^{-4} mol) of Na_2CO_3, 0.017 g (1.25×10^{-4} mol) of SnO, 1.056 g (6.00×10^{-3} mol) of HIO_3, and 2 mL of deionized water were combined. The respective mixtures were transferred into 23 mL Teflon-lined stainless steel autoclaves. After sealing, the autoclaves were gradually heated to 230 ℃ for 4 days, before being cooled to room temperature at a rate of 6 ℃ h^{-1}. After cooling, the autoclaves were opened and the products were recovered by filtration and washed with water. Colorless crystals of $Li_2Sn(IO_3)_6$, $Na_2Sn(IO_3)_6$, $K_2Sn(IO_3)_6$, $Rb_2Sn(IO_3)_6$, and $Cs_2Sn(IO_3)_6$ were obtained in 54%, 46%, 78%, 72%, and 85% yields, respectively, based on $SnCl_2$. Although several attempts have been made, we were not able to synthesize a pure phase of $Sn^{2+}Sn^{4+}(IO_3)_6$. A few colorless cube crystals of $Sn^{2+}Sn^{4+}(IO_3)_6$ were manually extracted from black plates crystals of SnO for single crystal X-ray diffraction. Thus, with $Sn^{2+}Sn^{4+}(IO_3)_6$, only the crystal structure will be given here. Powder X-ray diffraction patterns on the bulk samples for other five compounds revealed that the synthesized materials are pure and in very good agreements with the generated patterns from the single-crystal data (see the ESI).

Single-crystal X-ray diffraction

The crystal structures of the reported materials were determined by a standard crystallographic method. A colorless rod ($0.018 \times 0.020 \times 0.073$ mm^3) for $Li_2Sn(IO_3)_6$, a colorless rod ($0.020 \times 0.020 \times 0.100$ mm^3) for $Na_2Sn(IO_3)_6$, a colorless cube ($0.036 \times 0.038 \times 0.038$ mm^3) for $K_2Sn(IO_3)_6$, a colorless cube ($0.030 \times 0.031 \times 0.031$ mm^3) for $Rb_2Sn(IO_3)_6$, a colorless cube ($0.031 \times 0.031 \times 0.032$ mm^3) for $Cs_2Sn(IO_3)_6$, and a colorless cube ($0.031 \times 0.031 \times 0.032$ mm^3) for $Sn^{2+}Sn^{4+}(IO_3)_6$ were used for single crystal X-ray diffraction analyses. Diffraction data were collected at room temperature using a Bruker SMART BREEZE diffractometer equipped with a 1K CCD area detector using graphite monochromated Mo Kα radiation. A narrow-frame method was used with an exposure time of 10 s/frame, and scan widths of 0.30° in omega to collect a hemisphere of data. The maximum correction applied to the intensities was < 1%. The data were integrated using the SAINT program,[37] with the intensities corrected for polarization, Lorentz factor, air absorption, and absorption attributed to the variation in the path length through the detector faceplate. The data were solved with SHELXS-97[38] and refined using SHELXL-97.[39] All calculations were performed using the WinGX-98 crystallographic software package.[40] Crystallographic data and selected bond distances for the reported materials are summarized in Tables 1 and 2, respectively.

Table1 Crystallographic data for $A_2Sn(IO_3)_6$ (A = Li, Na, K, Rb, Cs) and $Sn^{2+}Sn^{4+}(IO_3)_6$

Formula	$Li_2Sn(IO_3)_6$	$Na_2Sn(IO_3)_6$	$K_2Sn(IO_3)_6$	$Rb_2Sn(IO_3)_6$	$Cs_2Sn(IO_3)_6$	$Sn_2(IO_3)_6$
Formula weight	1181.99	1214.09	1246.31	1339.05	1433.93	1286.82
Crystal system	Hexagonal	Hexagonal	Trigonal	Trigonal	Trigonal	Trigonal
Space group	$P6_3$ (No. 173)	$P6_3$ (No. 173)	R-3 (No. 148)	R-3 (No. 148)	R-3 (No. 148)	R-3 (No. 148)
$a = b$/Å	9.4532(10)	9.7154(10)	11.3300(10)	11.5049(10)	11.7196(10)	11.3779(10)
c/Å	5.1680(3)	5.2239(10)	11.3841(10)	11.4933(10)	11.7232(10)	11.2743(2)
V/Å^3	399.96(13)	427.02(14)	1265.6(3)	1318.2(3)	1394.5(3)	1264.0(3)
Z	1	1	3	3	3	3
T/K	298.0(2)	298.0(2)	298.0(2)	298.0(2)	298.0(2)	298.0(2)
λ/Å	0.71073	0.71073	0.71073	0.71073	0.71073	0.71073
$R(F)^a$	0.0405	0.0593	0.0129	0.0189	0.0138	0.0279
$R_w(F_o^2)^b$	0.1024	0.1454	0.0295	0.0454	0.0248	0.0677
Flack parameter	0.01(4)	0.08(3)	N/A	N/A	N/A	N/A

$^a R(F)=\Sigma||F_o| - |F_c|| / \Sigma |F_o|$.

$^b R_w(F^2) = [\Sigma w(F_o^2 - F_c^2)^2 / \Sigma w(F_o^2)^2]^{1/2}$.

Table 2 Selected bond distances (Å) for $A_2Sn(IO_3)_6$ (A = Li, Na, K, Rb, Cs) and $Sn^{2+}Sn^{4+}(IO_3)_6$

bond	$Li_2Sn(IO_3)_6$	$Na_2Sn(IO_3)_6$
Sn(1)–O(1) × 3	2.070(19)	2.10(3)
Sn(1)–O(1) × 3	2.115(18)	2.14(3)
I(1)–O(1)	1.875(19)	1.87(3)
I(1)–O(2)	1.798(16)	1.77(3)
I(1)–O(3)	1.791(17)	1.80(2)
A(1)–O(2) × 3	2.11(3)	2.28(2)
A(1)–O(3) × 3	2.25(3)	2.42(3)

bond	$K_2Sn(IO_3)_6$	$Rb_2Sn(IO_3)_6$	$Cs_2Sn(IO_3)_6$	$SnSn(IO_3)_6$
Sn(1)–O(1) × 6	2.0434(19)	2.038(3)	2.037(2)	2.034(6)
I(1)–O(1)	1.8653(19)	1.864(3)	1.853(2)	1.856(6)
I(1)–O(2)	1.799(2)	1.804(3)	1.796(2)	1.806(5)
I(1)–O(3)	1.7964(19)	1.788(3)	1.782(2)	1.787(5)
A(1)–O(1) × 3	2.934(2)	3.016(3)	3.117(2)	3.142(6)
A(1)–O(2) × 3	2.868(2)	2.988(3)	3.142(2)	2.878(5)
A(1)–O(3) × 3	2.921(2)	3.004(3)	3.149(2)	2.827(6)

Powder X-ray diffraction (PXRD)

PXRD data were obtained using a Bruker D8-Advance diffractometer (Cu Kα radiation). The diffraction data were collected at room temperature with 40 kV and 40 mA. The ground samples were mounted on sample holders and scanned in the 2θ range 5–70° with a step size of 0.02° and a step time of 0.2 s.

Infrared (IR) spectroscopy

IR spectra were obtained on a Thermo Scientific Nicolet 6700 FT-IR spectrometer in the spectral range 400–4000 cm^{-1}. The samples were embedded in KBr matrixes for the measurements.

UV-vis spectroscopy

UV-vis diffuse reflectance spectra were obtained on a Varian Cary 500 scan UV-vis-NIR spectrophotometer equipped with a double-beam photomultiplier tube in the range of 200–1500 nm at room temperature.

Thermogravimetric analysis (TGA)

TGA was performed on a Setaram LABSYS TG-DTA thermogravimetric analyser. The samples were contained in alumina crucibles and heated to 1000 °C at a rate of 10 °C min^{-1} under flowing argon.

Scanning electron microscope (SEM)/energy-dispersive analysis by X-ray (EDAX)

SEM/EDAX analyses were conducted by Hitachi S-3400N/Horiba energy EX-250 instruments. EDAX for $A_2Sn(IO_3)_6$ (A = Li, Na, K, Rb, Cs) reveal A:Sn:I ratios of approximately N/A:1.0:5.6, 1.9:1.0:5.9, 1.8:1.0:6.2, 1.7:1.0:6.2, and 2.0:1.0:5.8, respectively.

Powder second-harmonic generation (SHG) measurements

Powder SHG measurements on polar NCS compounds, $Li_2Sn(IO_3)_6$ and $Na_2Sn(IO_3)_6$ were performed on a modified Kurtz NLO system[41] using 1064 nm radiation using a DAWA Q-switched Nd:YAG laser operating at 20 Hz. SHG efficiencies for polycrystalline samples have been known to depend on particle size; thus, powder samples were graded into distinct ranges of particle size. To compare suitably with known SHG materials, crystalline α-SiO_2 and $LiNbO_3$ were also sieved into the same particle size ranges. Samples with particle size range of 45–63 μm were used to compare SHG efficiencies. Polycrystalline samples with different particle size ranges were placed in individual capillary tubes. The frequency-doubled SHG light, 532 nm green, was gathered and detected by a photomultiplier tube (PMT, Hamamatsu). A narrow-pass interference filter (532 nm) was attached to the PMT to detect only the SHG light. To monitor the SHG signal, a digital oscilloscope (Tektronix TDS1032) was connected. A detailed description of the equipment and the methodology has been published.[42]

Piezoelectric measurements

Converse piezoelectric measurements were performed using a Radiant Technologies RT66A piezoelectric test system with a TREK (model 609E–6) high-voltage amplifier, Precision Materials Analyzer, Precision High-Voltage Interface, and MTI 2000 Fotonic Sensor. NCS $Na_2Sn(IO_3)_6$ was pressed into a 12 mm diameter and ~0.8 mm thick pellet and sintered at 300 °C for 6 h. A conducting solver paste was applied on both sides of the pellet surfaces for electrodes. A maximum voltage of 500 V was applied to the sample.

Polarization measurements

The polarization measurements were carried out on a Radiant Technologies RT66A ferroelectric test system with a TREK high-voltage amplifier between room temperature and 200 °C in a Delta 9023 environmental test chamber. The unclamped pyroelectric coefficient, d*P*/d*T*, was determined by measuring the polarization (*P*) as a function of temperature (*T*). A detailed statement of the methodology used has been reported.[42] The same pellet of $Na_2Sn(IO_3)_6$ used for piezoelectric measurements was utilized for polarization measurements. To determine the ferroelectric behaviour, polarization measurements were done at room temperature under a static electric field of 15.0 kV/cm at frequencies ranging 100–1000 Hz. For the pyroelectric measurements, the polarization was measured statically from room temperature to 200 °C in 20 °C increments, with an electric field of 15.0 kV/cm. The temperature was allowed to stabilize before the polarization was measured.

Results and discussion

Crystal structures

All six stoichiometrically similar tin iodates exhibit zero-dimensional structures that are composed of SnO_6 octahedra and IO_3 groups (see Fig. 1).

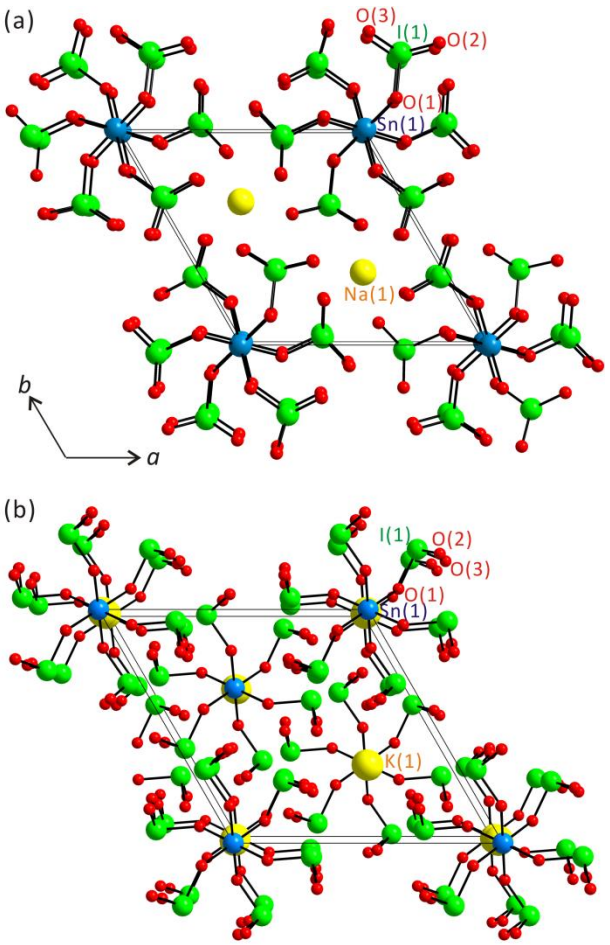

Fig.1 Ball-and-stick models for (a) NCS polar $Na_2Sn(IO_3)_6$ and (b) CS nonpolar $K_2Sn(IO_3)_6$ in the *ab*-plane.

As seen in Fig.1, the large molecular groups of SnO_6 and IO_3 polyhedra are kept apart by alkali metal or Sn^{2+} cations. Thus, the reported materials share a general connectivity term of $\{[SnO_{6/2}]^{2-}\ 6[IO_{1/2}O_{2/1}]^0\}^{2-}$, with charge balance retained by two alkali metal cations or a Sn^{2+} cation. Interestingly, however, while $Li_2Sn(IO_3)_6$ and $Na_2Sn(IO_3)_6$ crystallize in NCS polar space group, $P6_3$ (No. 173), $A_2Sn(IO_3)_6$ (A = K, Rb, Cs) and $Sn^{2+}Sn^{4+}(IO_3)_6$ crystallize in CS nonpolar space group, R-3 (No. 148). The Sn^{4+} cations in NCS $Li_2Sn(IO_3)_6$ and $Na_2Sn(IO_3)_6$ reveal C_3-type distortions and result in three short and three long Sn–O bonds. Here the Sn^{4+} cation is disordered over two sites with 50% occupancy on each site, which makes the materials effectively 0-dimensional molecular structures. Similar disordered structures have been observed from polar titanium iodates.[28, 29] The observed Sn–O bond lengths for $Li_2Sn(IO_3)_6$ and $Na_2Sn(IO_3)_6$ are 2.070(19)–2.115(18) Å and 2.10(3)–2.14(3) Å, respectively. The I^{5+} cations in $Li_2Sn(IO_3)_6$ and $Na_2Sn(IO_3)_6$ are in asymmetric trigonal pyramidal environment attributed to their stereoactive lone pairs. The I–O bond distances for $Li_2Sn(IO_3)_6$ and $Na_2Sn(IO_3)_6$ range from 1.791(17) to 1.875(19) Å and from 1.77(3) to 1.87(3) Å, respectively. The Li^+ and Na^+ cations are in pseudo-octahedral coordination moieties with six oxygen ligands with bond lengths in the range 2.11(3)–2.42(3) Å. With CS $A_2Sn(IO_3)_6$ (A = K, Rb, Cs) and $Sn^{2+}Sn^{4+}(IO_3)_6$, the Sn^{4+} cations are in the center of their normal octahedra with one unique Sn–O bond lengths of approximately 2.04 Å. Similar to those of $Li_2Sn(IO_3)_6$ and $Na_2Sn(IO_3)_6$, each I^{5+} cation in CS $A_2Sn(IO_3)_6$ and $Sn^{2+}Sn^{4+}(IO_3)_6$ is linked to three oxygen atoms in a trigonal pyramidal environment with the I–O bond lengths in the approximate range 1.78–1.87 Å (see Table 2). The K^+, Rb^+, Cs^+, and Sn^{2+} in CS tin iodates are in ninefold coordination environments with contact distances in the range 2.827(6)–3.149(2) Å. Similar coordination moieties for the CS tin iodates strongly indicate that the materials are isostructural to each other and the lone pair on Sn^{2+} is not stereoactive but inert. Similar inertness of the lone pair cations have been observed previously in other materials.[29, 43, 44] Bond valence sum calculations[45, 46] for the alkali-metal cations, Sn^{2+}, Sn^{4+}, and I^{5+} on the reported tin iodates resulted in values of 0.90–1.26, 2.05, 3.70–4.15, and 4.93–5.03, respectively.

As can be seen in Fig. 2, all of the lone pairs on the iodates are aligned in a parallel manner in $Li_2Sn(IO_3)_6$ and $Na_2Sn(IO_3)_6$, in which a produced macroscopic dipole moment makes the materials crystallographic polar. However, in $A_2Sn(IO_3)_6$ (A = K, Rb, Cs) and $Sn^{2+}Sn^{4+}(IO_3)_6$, the lone pairs on iodate polyhedra positioned *trans* to each other are oriented in opposite directions (see Fig. 3), which results in a complete cancellation of the polarization generated from the local dipole moments. Thus, the materials crystallize in the CS nonpolar space group.

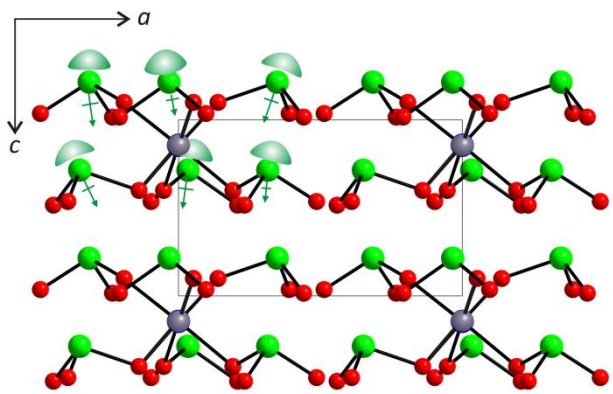

Fig. 2 Ball-and-stick representation of $Na_2Sn(IO_3)_6$ in the *ac*-plane. Note the lone pairs on the iodates are aligned in a parallel manner and a net moment is produced along the [001] direction. Lone pairs on I^{5+} cations are drawn schematically and not the result of the electron localization function (ELF) calculations.

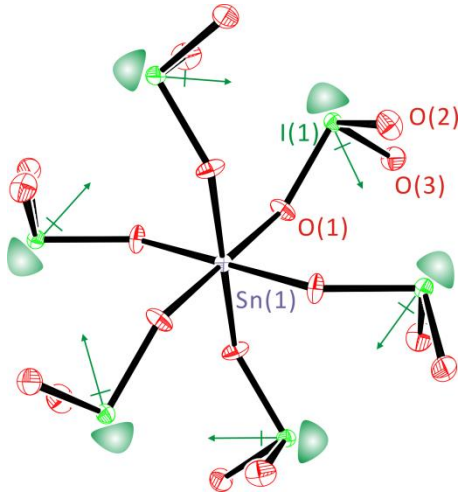

Fig.3 ORTEP (50% probability ellipsoids) drawing of $Cs_2Sn(IO_3)_6$. Note the lone pairs on iodate polyhedra positioned *trans* to each other are oriented in opposite directions, which results in a complete cancellation of the polarization and macroscopic CS. Lone pairs on I^{5+} cations are drawn schematically and not the result of the electron localization function (ELF) calculations.

IR spectroscopy

The reported tin iodate compounds reveal Sn–O and I–O vibrations in the IR spectra. The Sn–O vibrations are found at ca. 660–663 cm^{-1}. The I–O stretching and bending are also observed around 709–824 and 426–497 cm^{-1}, respectively. The assignments are consistent with those previous published.[47-49] The IR spectra are given in the ESI.

UV-vis diffuse reflectance spectroscopy

UV-vis diffuse reflectance spectra were obtained for the reported tin iodates. Absorption (*K*/*S*) data were calculated from the Kubelka-Munk function:[50, 51]

$$F(R) = \frac{(1-R)^2}{2R} = \frac{K}{S}$$

in which *S* is the scattering, *K* is the absorption, and *R* is the reflectance. In the *K*/*S* vs. *E* plots, extrapolating the linear part of the rising curve to zero yielded the onset of absorption at 3.9, 4.0, 4.0, 4.1, and 4.1 eV for $Li_2Sn(IO_3)_6$, $Na_2Sn(IO_3)_6$, $K_2Sn(IO_3)_6$, $Rb_2Sn(IO_3)_6$, and $Cs_2Sn(IO_3)_6$, respectively (see the ESI). The band gaps for the reported compounds are attributed to the interaction of the Sn–O and I–O bonds and the distortions arising from IO_3 groups.

Thermogravimetric analysis (TGA)

The thermal behaviors of the reported materials were investigated using TGA. TGA measurements showed that the materials decompose above 400 °C. Powder XRD for the thermally decomposed products revealed SnO_2 and alkali metal tin oxides. The TGA diagrams are found in the ESI.

Noncentrosymmetric (NCS) properties

$Li_2Sn(IO_3)_6$ and $Na_2Sn(IO_3)_6$, crystallize in the NCS polar space group, $P6_3$; thus, their SHG properties have been investigated. The SHG efficiencies of the NCS tin iodates are very strong; both $Li_2Sn(IO_3)_6$ and $Na_2Sn(IO_3)_6$ exhibit SHG efficiencies of ~400 times that of α-SiO_2, which compares well to $BaTiO_3$ (400 times that of α-SiO_2).[41] The SHG efficiencies for alkali metal titanium iodates, $Li_2Ti(IO_3)_6$ and $Na_2Ti(IO_3)_6$, are ~500 and ~400 times that of α-SiO_2, respectively.[28, 29] The larger SHG efficiency of $Li_2Ti(IO_3)_6$ compared to that of $Li_2Sn(IO_3)_6$ may be attributed to the constructive addition of polarizations from both TiO_6 and IO_3 polyhedra. Overall, the similar efficiencies strongly indicate that the SHG for the iodates are mainly attributable to the alignment of the dipole moments in the IO_3 groups (see Fig. 2 and dipole moment calculations section). In addition, we were able to determine the type I phase-matching capabilities for the NCS polar materials by sieving them into various particle sizes and measuring the SHG as a function of particle size. As seen in Fig. 4, both $Li_2Sn(IO_3)_6$ and $Na_2Sn(IO_3)_6$ are phase-matchable and can be classified as the class A category of SHG materials, as defined by Kurtz and Perry.[41]

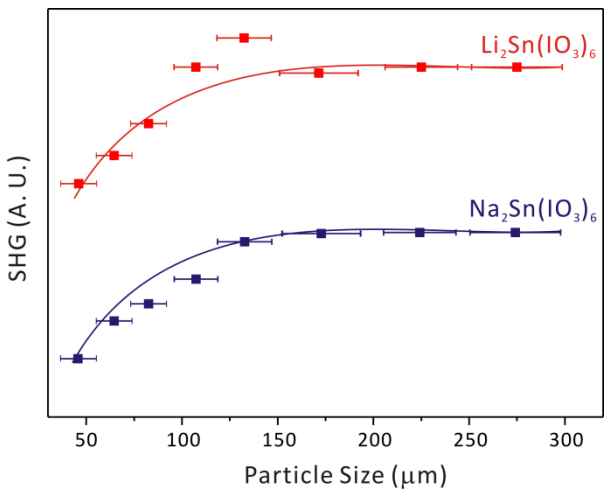

Fig. 4 Phase matching curve (Type I) for $Li_2Sn(IO_3)_6$ and $Na_2Sn(IO_3)_6$. The curves are to guide the eye and are not fit to the data.

Converse piezoelectric measurements on bulk $Na_2Sn(IO_3)_6$ revealed a d_{33} charge constant of 29.2 pm/V (see the ESI). The value compares well to that for other iodates, *i.e.*, KIO_3 (d_{33} = 39 pm/V) and $Na_2Ti(IO_3)_6$ (d_{33} = 60 pm/V).[29, 52] Ferroelectric and pyroelectric measurements for $Na_2Sn(IO_3)_6$ were also performed. Although the material is polar, $Na_2Sn(IO_3)_6$ is not ferroelectric as can be seen in the ferroelectric measurements (see the ESI). Polarization measurements using 15 kV/cm indicated an induced maximum polarization of only 0.07 $\mu C/cm^2$. In order to be ferroelectric, the dipole moment needs to be reversible. In $Na_2Sn(IO_3)_6$, the distortion associated with

Sn^{4+} is negligible, as we will discuss more in detail later (see dipole moment calculations section). With I^{5+} in the IO_3 polyhedron in an extended solid-state structure, the macroscopic polarization cannot be switched in the presence of an external electric field, because polarization reversal for the lone pair cation is extremely unfavorable. The energetically very unfavorable polarization reversal of the IO_3 polyhedra has been demonstrated before through calculations.[29] Although $Na_2Sn(IO_3)_6$ is not ferroelectric, the compound is pyroelectric. Thus, the pyroelectric coefficient for $Na_2Sn(IO_3)_6$ has been determined by measuring the polarization between room temperature and 200 °C, with an external electric field of 15.0 kV/cm. The obtained pyroelectric coefficients is approximately 0.5 μC m^{-2} K^{-1}, which is similar to that of sodium titanium iodate, $Na_2Ti(IO_3)_6$ (0.8 μC m^{-2} K^{-1}).[29]

Dipole moment calculations

The reported stoichiometrically similar compounds contain asymmetric polyhedra, *i.e.*, IO_3 groups attributed to the lone pairs. Thus, the asymmetric environment of the IO_3 polyhedra has been quantified through local dipole moment calculations using the method described before.[8, 9, 53] The distortion of SnO_6 octahedra has been also calculated for comparison. We found that the local dipole moments for IO_3 and SnO_6 groups in $A_2Sn(IO_3)_6$ (A = Li, Na, K, Rb, Cs) are calculated to be about 13.1–13.9 and 0–0.4 D (Debyes), respectively, which are very similar values to those of previously reported iodate materials.[28, 29, 49] As we described earlier, while the polarization arising from the distortion of SnO_6 octahedra is negligible, the polarization associated with IO_3 polyhedra is significant. Thus, the functional properties for NCS polar materials are attributed to a net moment originated from the alignment of IO_3 groups. The local dipole moments for the IO_3 and SnO_6 groups are summarized in Table 3.

Table 3 Calculation of dipole moments for IO_3 and SnO_6 polyhedra in $A_2Sn(IO_3)_6$ (A = Li, Na, K, Rb, Cs). D = Debyes

Compound	Species	Dipole moment (D)
$Li_2Sn(IO_3)_6$	$I(1)O_3$	13.2
	$Sn(1)O_6$	0.4
$Na_2Sn(IO_3)_6$	$I(1)O_3$	13.1
	$Sn(1)O_6$	0.3
$K_2Sn(IO_3)_6$	$I(1)O_3$	13.5
	$Sn(1)O_6$	0
$Rb_2Sn(IO_3)_6$	$I(1)O_3$	13.2
	$Sn(1)O_6$	0
$Cs_2Sn(IO_3)_6$	$I(1)O_3$	13.9
	$Sn(1)O_6$	0

NCS polar vs. CS nonpolar structures

Although all six stoichiometrically similar materials, $A_2Sn(IO_3)_6$ (A = Li, Na, K, Rb, Cs) and $Sn^{2+}Sn^{4+}(IO_3)_6$, share a molecular structure consisting of SnO_6 octahedra and IO_3 polyhedra, an interesting change in macroscopic polarity occurs from the NCS polar structure for the compounds containing smaller cations, Li^+ and Na^+, to the CS nonpolar structure for those with larger cations, K^+, Rb^+, Cs^+, and Sn^{2+}. With $Li_2Sn(IO_3)_6$ and $Na_2Sn(IO_3)_6$, the alkali metal cations, Li^+ and Na^+ are in six-coordinate pseudo-octahedral coordination environment attributed to their smaller cation size. To maintain this octahedral coordination mode around the Li^+ and Na^+ cations, the IO_3 groups should be aligned in a parallel manner around the Sn^{4+} cation, which subsequently results in a NCS polar structure (see Fig. 5a). It should be noted, however, that this parallel alignment in the crowded environment is only possible when the ionic radii of the cations are small. Whereas, the cations, K^+, Rb^+, Cs^+, and Sn^{2+} in CS nonpolar structures maintain nine-coordinate environments with oxide ligands attributable to the larger ionic radii (see Fig. 5b). As seen in Fig. 5b, the larger A^+ cations can have nine oxide contacts by rotating the IO_3 polyhedra with respect to the Sn^{4+} cation. Thus, the local dipole moments for IO_3 polyhedra point in opposite directions equally and render the material CS nonpolar. Similar cation size effect on the coordination environments and macroscopic centricity has been observed before.[29, 54, 55]

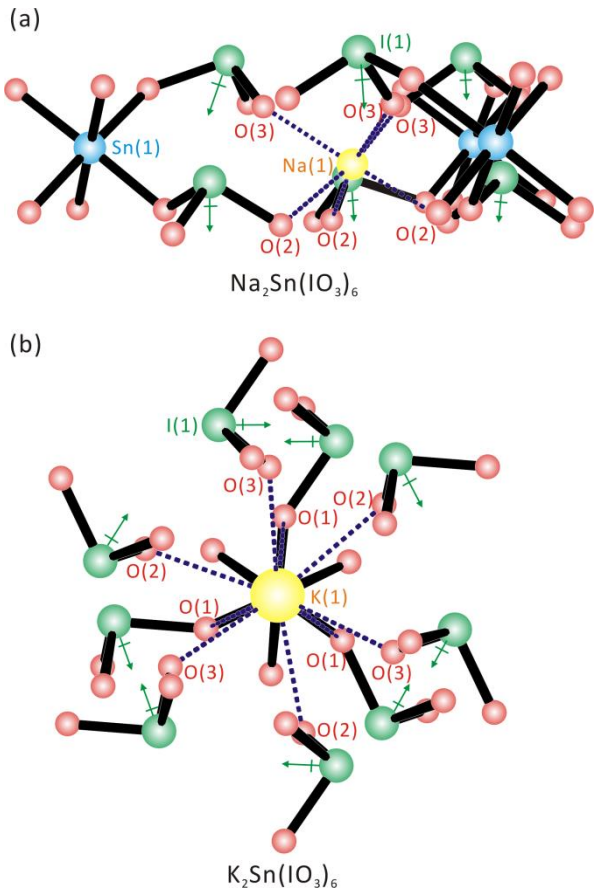

Fig. 5 Ball-and-stick representations for (a) NCS $Na_2Sn(IO_3)_6$ and (b) CS $K_2Sn(IO_3)_6$, with the alkali metal coordination environments emphasized. Note the IO_3 groups in $Na_2Sn(IO_3)_6$ are aligned in a parallel manner attributed to the six-coordinate Na^+ cation, whereas the IO_3 polyhedra in $K_2Sn(IO_3)_6$ rotate with respect to Sn^{4+} due to nine-coordinate K^+ cation.

Conclusions

Six new tin iodates, $A_2Sn(IO_3)_6$ (A = Li, Na, K, Rb, Cs) and $Sn^{2+}Sn^{4+}(IO_3)_6$, have been synthesized hydrothermally and their structures were determined through single crystal X-ray diffraction. All six stoichiometrically similar tin iodates exhibit molecular structures that are composed of SnO_6 octahedra and IO_3 groups. While the compounds containing smaller cations, Li^+ and Na^+, are NCS polar, those with the larger cations, K^+, Rb^+, Cs^+, and Sn^{2+}, are CS nonpolar. The smaller alkali metal cations, Li^+ and Na^+, are in six-coordinate pseudo-octahedral coordination moiety and contact with oxide ligands on six different IO_3 groups. The compact interactions demand the lone pairs in IO_3 groups to align in a parallel manner and let $Li_2Sn(IO_3)_6$ and $Na_2Sn(IO_3)_6$ crystallize in the NCS polar space group. The larger cations, K^+, Rb^+, Cs^+, and Sn^{2+}, interact with oxide ligands on IO_3 and SnO_6 groups in nine-coordinate environments. To maintain these contacts, the IO_3 polyhedra should rotate with respect to the SnO_6 octahedron, in which the rotation aligns the polarizations from the IO_3 groups in opposite directions. Thus, all tin iodates with larger cations, $K_2Sn(IO_3)_6$, $Rb_2Sn(IO_3)_6$, $Cs_2Sn(IO_3)_6$, and $Sn^{2+}Sn^{4+}(IO_3)_6$ crystallize in the CS nonpolar space group. The NCS functional properties such as SHG, piezoelectricity, and pyroelectricity are attributable to the parallel alignment of the lone pairs on the I^{5+} cations.

Acknowledgements

This research was supported by the National Research Foundation of Korea (NRF) funded by the Korea government (MSIP) (grants: 2013R1A2A2A01007170 and 2014M3A9B8023478). TTT and PSH thank the Welch Foundation (E-1457) for support.

Notes and references

[1,*]*Department of Chemistry, Chung-Ang University, 84 Heukseok-ro, Dongjak-gu, Seoul 156-756, Republic of Korea. Fax: 82 8 825 4735; Tel: 82 2 820 5197; E-mail: kmok@cau.ac.kr.* [2]*Department of Chemistry, University of Houston, 112 Fleming Building, Houston, TX 77204-5003, USA.*

†Electronic Supplementary Information (ESI) available: X-ray crystallographic file in CIF format, calculated and observed X-ray diffraction patterns, TGA diagrams, IR spectra, UV-vis diffuse reflectance spectra, piezoelectric, polarization, and pyroelectric measurements data. CCDC 1041408–1041413. For ESI and crystallographic data in CIF or other electronic forma see DOI: 10.1039/b000000x/

1. D. W. Bruce, D. O'Hare and R. I. Walton, *Molecular Materials*, John Wiley & Son, Ltd., West Sussex, U.K., 2010.
2. P. S. Halasyamani and K. R. Poeppelmeier, *Inorg. Chem.*, 2008, **47**, 8427.
3. M. E. Lines and A. M. Glass, *Principles and Applications of Ferroelectrics and Related Materials*, Oxford University Press, Oxford, U.K., 1991.
4. S. B. Lang and D. K. Das-Gupta, *Handbook of Advanced Electronic and Photonic Materials and Devices*, Academic Press, San Francisco, USA, 2001.
5. T. Hahn, *International Tables for Crystallography, Volume A: Space Group Symmetry*, Kluwer Academic, Dordrecht, The Netherlands, 2006.
6. P. A. Maggard, C. L. Stern and K. R. Poeppelmeier, *J. Am. Chem. Soc.*, 2001, **123**, 7742.
7. M. E. Welk, A. J. Norquist, F. P. Arnold, C. L. Stern and K. R. Poeppelmeier, *Inorg. Chem.*, 2002, **41**, 5119.
8. P. A. Maggard, T. S. Nault, C. L. Stern and K. R. Poeppelmeier, *J. Solid State Chem.*, 2003, **175**, 27.
9. H. K. Izumi, J. E. Kirsch, C. L. Stern and K. R. Poeppelmeier, *Inorg. Chem.*, 2005, **44**, 884.
10. M. R. Marvel, J. Lesage, J. Baek, P. S. Halasyamani, C. L. Stern and K. R. Poeppelmeier, *J. Am. Chem. Soc.*, 2007, **129**, 13963.
11. U. Opik and M. H. L. Pryce, *Proc. R. Soc. London*, 1957, **A238**, 425.
12. R. F. W. Bader, *Mol. Phys.*, 1960, **3**, 137.
13. R. F. W. Bader, *Can. J. Chem.*, 1962, **40**, 1164.
14. R. G. Pearson, *J. Am. Chem. Soc.*, 1969, **91**, 4947.
15. R. G. Pearson, *J. Mol. Struct.: THEOCHEM*, 1983, **103**, 25.
16. R. A. Wheeler, M.-H. Whangbo, T. Hughbanks, R. Hoffmann, J. K. Burdett and T. A. Albright, *J. Am. Chem. Soc.*, 1986, **108**, 2222.
17. J. B. Goodenough, *Annu. Rev. Mater. Sci.*, 1998, **28**, 1.
18. H.-S. Ra, K. M. Ok and P. S. Halasyamani, *J. Am .Chem. Soc.*, 2003, **125**, 7764.
19. E. O. Chi, K. M. Ok, Y. Porter and P. S. Halasyamani, *Chem. Mater.*, 2006, **18**, 2070.
20. H. Jiang, S. Huang, Y. Fan, J.-G. Mao and W. Cheng, *Chem.–Eur. J.*, 2008, **14**, 1972.
21. C.-F. Sun, C.-L. Hu, X. Xu, J.-B. Ling, T. Hu, F. Kong, X.-F. Long and J.-G. Mao, *J. Am. Chem. Soc.*, 2009, **131**, 9486.
22. C. Huang, C.-L. Hu, X. Xu, B.-P. Yang and J.-G. Mao, *Dalton Trans.*, 2013, **42**, 7051.
23. S. Pan, J. P. Smit, B. Watkins, M. R. Marvel, C. L. Stern and K. R. Poeppelmeier, *J. Am. Chem. Soc.*, 2006, **128**, 11631.
24. Y. Inaguma, M. Yoshida and T. Katsumata, *J. Am. Chem. Soc.*, 2008, **130**, 6704.
25. H. Wu, H. Yu, Z. Yang, X. Hou, X. Su, S. Pan, K. R. Poeppelmeier and J. M. Rondinelli, *J. Am. Chem. Soc.*, 2013, **135**, 4215.
26. H. Yu, S. Pan, H. Wu, Z. Yang, L. Dong, X. Su, B. Zhang and H. Li, *Cryst. Growth Des.*, 2013, **13**, 3514.
27. X. Lin, F. Zhang, S. Pan, H. Yu, F. Zhang, X. Dong, S. Han, L. Dong, C. Bai and Z. Wang, *J. Mater. Chem. C.*, 2014, **2**, 4257.
28. H.-Y. Chang, S.-H. Kim, P. S. Halasyamani and K. M. Ok, *J. Am. Chem. Soc.*, 2009, **131**, 2426.
29. H.-Y. Chang, S.-H. Kim, K. M. Ok and P. S. Halasyamani, *J. Am. Chem. Soc.*, 2009, **131**, 6865.
30. C.-F. Sun, G.-L. Hu, F. Kong, B.-P. Yang and J.-G. Mao, *Dalton Trans.*, 2010, **39**, 1473.
31. R. E. Sykora, K. M. Ok, P. S. Halasyamani and T. E. Albrecht-Schmitt, *J. Am .Chem. Soc.*, 2002, **124**, 1951.

32. J. Goodey, K. M. Ok, J. Broussard, C. Hofmann, F. V. Escobedo and P. S. Halasyamani, *J. Solid State Chem.*, 2003, **175**, 3.
33. K. M. Ok, J. Baek, P. S. Halasyamani and D. O'Hare, *Inorg. Chem.*, 2006, **45**, 10207.
34. M.-H. Choi, S.-H. Kim, H. Y. Chang, P. S. Halasyamani and K. M. Ok, *Inorg. Chem.*, 2009, **48**, 8376.
35. D. W. Lee, S. J. Oh, P. S. Halasyamani and K. M. Ok, *Inorg. Chem.*, 2012, **50**, 4473.
36. Y. H. Kim, D. W. Lee and K. M. Ok, *Inorg. Chem.*, 2014, **53**, 1250.
37. *SAINT, Program for Area Detector Absorption Correction*; *version 4.05;* Siemens Analytical X-ray Instruments: Madison, WI, USA, 1995.
38. G. M. Sheldrick, *SHELXS-97 - A program for automatic solution of crystal structures*; University of Goettingen: Goettingen, Germany, 1997.
39. G. M. Sheldrick, *SHELXL-97 - A program for crystal structure refinement*; University of Goettingen: Goettingen, Germany, 1997.
40. L. J. Farrugia, *J. Appl. Crystallogr.*, 1999, **32**, 837.
41. S. K. Kurtz and T. T. Perry, *J. Appl. Phys.*, 1968, **39**, 3798.
42. K. M. Ok, E. O. Chi and P. S. Halasyamani, *Chem. Soc. Rev.*, 2006, **35**, 710.
43. A.-V. Mudring, *Eur. J. Inorg. Chem.*, 2007, 882.
44. F. Rieger and A.-V. Mudring, *Inorg. Chem.*, 2007, **46**, 446.
45. I. D. Brown and D. Altermatt, *Acta Crystallogr.*, 1985, **B41**, 244.
46. N. E. Brese and M. O'Keeffe, *Acta Crystallogr.*, 1991, **B47**, 192.
47. M. C. F. Alves, S. C. Souza, M. R. S. Silva, E. C. Paris, S. J. G. Lima, R. M. Gomes, E. Longo, A. G. d. Souza and I. M. G. d. Santos, *J. Therm. Anal. Calorim.*, 2009, **97**, 179.
48. E. Moreira, J. M. Henriques, D. L. Azevedo, E. W. S. Caetano, V. N. Freire and E. L. Albuquerque, *J. Solid State Chem.*, 2011, **184**, 921.
49. D. W. Lee, S. B. Kim and K. M. Ok, *Dalton Trans.*, 2012, **41**, 8348.
50. P. Kubelka and F. Munk, *Z. Tech. Phys.* , 1931, **12**, 593.
51. J. Tauc, *Mater. Res. Bull.*, 1970, **5**, 721.
52. H. Landolt, *Numerical Values and Functions from the Natural Sciences and Technology (New Series), Group 3: Crystal and Solid State Physics*, Springer Verlag, Berlin, Germany, 1979.
53. J. Galy and G. Meunier, *J. Solid State Chem.*, 1975, **13**, 142.
54. S.-J. Oh, D. W. Lee and K. M. Ok, *Inorg. Chem.*, 2012, **51**, 5393.
55. S.-e. Bang, D. W. Lee and K. M. Ok, *Inorg. Chem.*, 2014, **53**, 4756.

